

# Synergistic innovations enabled the radiation of anglerfishes in the deep open ocean

## Highlights

- Resolution of anglerfish phylogeny
- Anglerfishes radiated into the midnight zone during an ancient climate crisis
- Complex assembly of anglerfish sexual parasitism
- Complex innovations sculpted the ecological transition of bathypelagic anglerfishes

## Authors

Chase D. Brownstein,  
Katerina L. Zapfe, Spencer Lott,  
Richard Harrington, Ava Ghezelayagh,  
Alex Dornburg, Thomas J. Near

## Correspondence

chase.brownstein@yale.edu

## In brief

Brownstein et al. reconstruct the evolutionary history of anglerfishes and show how complex trait evolution, including the origins of sexual parasitism, facilitated the invasion of this clade into the deep open ocean where they diversified in the midst of a major climate change event.

## Report

# Synergistic innovations enabled the radiation of anglerfishes in the deep open ocean

Chase D. Brownstein,<sup>1,6,7,\*</sup> Katerina L. Zapfe,<sup>2</sup> Spencer Lott,<sup>1</sup> Richard Harrington,<sup>3</sup> Ava Ghezelayagh,<sup>4</sup> Alex Dornburg,<sup>2</sup> and Thomas J. Near<sup>1,5</sup>

<sup>1</sup>Department of Ecology and Evolutionary Biology, Yale University, 21 Sachem Street, New Haven, CT 06511, USA

<sup>2</sup>Department of Bioinformatics and Genomics, University of North Carolina Charlotte, 9331 Robert D. Snyder Rd., Charlotte, NC 28223, USA

<sup>3</sup>Department of Natural Resources, Marine Resources Division, 217 Ft. Johnson Road, Charleston, SC 29412-9110, USA

<sup>4</sup>Department of Geophysical Sciences, University of Chicago, 5734 S. Ellis Avenue, Chicago, IL 60637, USA

<sup>5</sup>Peabody Museum, Yale University, 21 Sachem Street, New Haven, CT 06511, USA

<sup>6</sup>X (formerly Twitter): [@ChaseBrownstein](#)

<sup>7</sup>Lead contact

\*Correspondence: [chase.brownstein@yale.edu](mailto:chase.brownstein@yale.edu)

<https://doi.org/10.1016/j.cub.2024.04.066>

## SUMMARY

Major ecological transitions are thought to fuel diversification, but whether they are contingent on the evolution of certain traits called key innovations<sup>1</sup> is unclear. Key innovations are routinely invoked to explain how lineages rapidly exploit new ecological opportunities.<sup>1–3</sup> However, investigations of key innovations often focus on single traits rather than considering trait combinations that collectively produce effects of interest.<sup>4</sup> Here, we investigate the evolution of synergistic trait interactions in anglerfishes, which include one of the most species-rich vertebrate clades in the bathypelagic, or “midnight,” zone of the deep sea: Ceratioidea.<sup>5</sup> Ceratioids are the only vertebrates that possess sexual parasitism, wherein males temporarily attach or permanently fuse to females to mate.<sup>6,7</sup> We show that the rapid transition of ancestrally benthic anglerfishes into pelagic habitats occurred during a period of major global warming 50–35 million years ago.<sup>8,9</sup> This transition coincided with the origins of sexual parasitism, which is thought to increase the probability of successful reproduction once a mate is found in the midnight zone, Earth’s largest habitat.<sup>5–7</sup> Our reconstruction of the evolutionary history of anglerfishes and the loss of immune genes support that permanently fusing clades have convergently degenerated their adaptive immunity. We find that degenerate adaptive immune genes and sexual body size dimorphism, both variably present in anglerfishes outside the ceratioid radiation, likely promoted their transition into the bathypelagic zone. These results show how traits from separate physiological, morphological, and reproductive systems can interact synergistically to drive major transitions and subsequent diversification in novel environments.

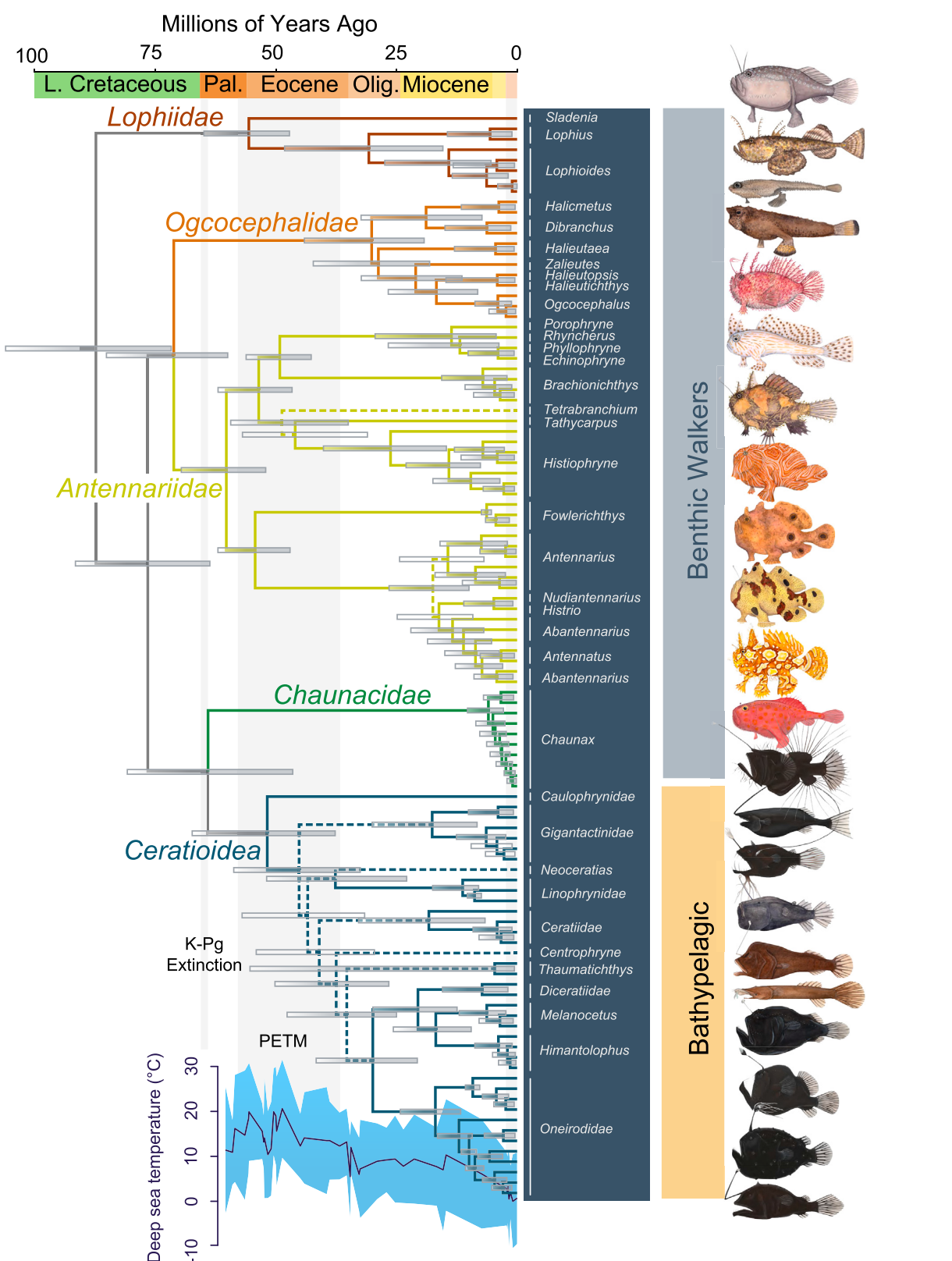
## RESULTS

### Genomic discordance stifles resolution of anglerfish evolutionary history

Phylogenetic relationships among the major lineages of anglerfishes have evaded resolution even in the era of widespread genome sequencing.<sup>10–15</sup> We inferred a time-calibrated phylogenomic tree of anglerfishes using a dataset of ultraconserved element (UCE) loci sequenced for 244 individuals, including 222 specimens of anglerfishes (*Lophioidei*) and 20 species of their sister lineage, the pufferfishes, ocean sunfishes, and triggerfishes (*Tetraodontoidei*). We employed a multistep bioinformatics pipeline<sup>16</sup> (see “method details”) to thoroughly scrutinize the 975 UCE sequences that we initially recovered, maximize alignment quality, and minimize the effects of known contributors to systematic error in phylogenetic inferences, such as hidden paralogy and model violations.<sup>17</sup> Using several tools (phyluce,<sup>16</sup> CIALign,<sup>18</sup> IQ-TREE2,<sup>19,20</sup> and TOAST<sup>21</sup>), we aligned and preprocessed UCE sequences, removed chimeric UCE sequence data,

*I guess this makes sense - otherwise I would expect the male flagged sequences that violated common molecular evolutionary model assumptions,<sup>22</sup> and removed aberrant gene trees generated from an initial run of UCE alignments in the likelihood-based phylogenetic software IQ-TREE2. These sanitation steps retained 608 UCE sequences. We estimated species trees based on the multispecies coalescent as implemented in ASTRAL-III<sup>23</sup> and used IQ-TREE2<sup>19</sup> to infer phylogenies from partitioned and concatenated versions of our UCE dataset.*

These UCE-inferred phylogenies resolve the deepest divergences in anglerfishes with strong support: goosefishes (*Lophiidae*) are the sister lineage of all other anglerfishes, batfishes (*Ogcocephalidae*) and the frogfishes and handfishes (*Antennariidae*) comprise a clade of benthic species with modified fins for walking along the seafloor,<sup>24</sup> and the seafloor-walking sea toads (*Chaunacidae*) are the sister lineage of the deep-sea anglerfishes (*Ceratioidea*) (Figure 1; Figures S1, S2, and S3). Our UCE phylogeny is comparable to the results of recent phylogenomic studies of anglerfishes<sup>10,12</sup> but differs considerably from efforts to resolve their relationships using smaller nuclear and mitochondrial



(legend on next page)

datasets<sup>13,25,26</sup> or morphological characters.<sup>27</sup> Our strongly supported inference of ceratioid monophyly (Figure 1) suggests that this lineage transitioned to open water habitats from an ancestor that used its pelvic fins to walk along the seafloor<sup>24</sup> in a manner reminiscent of major transitions at the origin of groups like whales and marine reptiles.<sup>28–30</sup>

Our results provide strongly supported resolution for the relationships of major lineages of anglerfishes. However, we find that a high degree of uncertainty underlies the relationships of major lineages of deep-sea ceratioids: the obligate sexual parasites in *Linophrynidae*, *Neoceratiias*, *Ceratiidae*, and *Centrophryne*, and the temporary attachers and facultative parasites in *Gigantactinidae*, *Thaumaticichthys*, *Himantolophus*, *Oneirodidae*, *Diceratiidae*, and *Melanocetus* (Figure 1; Figures S1, S2, and S3). The extensive phylogenetic discordance among individual loci indicates that the backbone of the ceratioid phylogeny is in the so-called anomaly zone (AZ) (Figure 1; Figures S4 and S5),<sup>17,31,32</sup> where variables such as large effective population size and rapid lineage divergence preclude adequate sorting of ancestral genetic variation and results in extensive incongruence among gene trees and the species tree. These results indicate that a rapid pace of lineage divergence underlies early ceratioid evolution.

### Anglerfishes radiated during a period of extreme oceanic warming

In order to investigate the tempo of anglerfish evolution, we time-calibrated the anglerfish tree by employing a Bayesian relaxed molecular clock model<sup>33</sup> with a partitioned UCE sequence dataset and a set of 13 fossil calibrations used as node calibrations (Figure 1). The ages estimated for the major anglerfish lineages, including an early Paleogene age for crown Ceratioidea,<sup>12</sup> are younger than previous estimates based on smaller phylogenetic datasets.<sup>13</sup> The median age of the most recent common ancestor (MRCA) of living anglerfishes is 87.7 Ma (95% highest posterior density interval [HPD]: 71.7, 106.0 Ma). All major living lineages of anglerfishes originated in the Cenozoic (Figure 1). The posterior median age of the MRCA of *Lophiidae* is 55.6 Ma (95% HPD: 46.5, 80.8 Ma); the *Antennariidae*, 60.3 Ma (95% HPD: 52.1, 69.6 Ma); and the *Ogcocephalidae*, 30.2 Ma (95% HPD: 19.3, 44.1 Ma). Sea toads (*Chaunacidae*) represent a recent (Figure S6) diversification with an MRCA age of 6.0 Ma (95% HPD: 2.8, 10.3 Ma; though note the genus *Chaunacops* is not included; see Figure S6). The common ancestry of ceratioid anglerfishes lies in the Paleocene-Eocene, 51.8 Ma (95% HPD: 37.7, 67.4 Ma). Nearly all ceratioid family-level clades diverged 50 to 30 million years ago (Figure 1) during the Paleocene-Eocene Thermal Maximum (PETM),<sup>8,34–37</sup> a period of high global temperatures that induced extinction throughout the world's oceans.<sup>34,38</sup> The rapid successive divergences of ceratioid clades (Figure 1) also correspond to a swift tempo of morphological evolution<sup>39</sup>

**Figure 1. Anglerfishes invaded and radiated in the deep sea during a global warming event**

Figure shows the Bayesian node-dated phylogeny produced from analysis of the 15 largest UCE partitions and 11 fossil calibrations in BEAST 2.6.6. Posterior tree sets generated from partitions that converged when analyzed were pooled and used to calibrate the target partitioned topology from IQ-TREE. Nodes are placed at median estimated ages, and gray bars at nodes indicate 95% highest posterior density intervals. Clear bars indicate bootstrap support values of less than 100 in the maximum likelihood tree resulting from analysis of the partitioned UCE dataset in IQ-TREE. Dotted branches indicate anomaly zones (AZs) in anglerfish phylogeny. L. Cretaceous denotes the Late Cretaceous, Pal. denotes the Paleocene, Olig. denotes the Oligocene, and PETM denotes the Paleocene-Eocene Thermal Maximum. Deep-sea temperature curve is from Meckler et al. Fish illustrations by Julie Johnson ([www.lifesciencestudios.com](http://www.lifesciencestudios.com)). Also see Data S1 and S2.

across the ceratioid backbone and confirm that the evolutionary history of deep-sea anglerfishes features classic signatures of adaptive radiation.<sup>3</sup>

### Ecological opportunity drove the adaptive radiation of ceratioid anglerfishes

What could have enabled deep-sea anglerfishes to make a major transition into water column habitats and diversify during a period of climate turmoil? To answer this question, we investigated the evolution of the unconventional physiology and behavior of anglerfish reproduction. The sexual parasitism of ceratioid anglerfishes is theorized to increase the chances of successful reproduction after finding a mate in the deep open ocean.<sup>5–7,11,40</sup> However, the association between reproductive mode and lineage diversification in anglerfishes has not been tested. Our analyses reveal significant associations between net lineage diversification and both reproductive mode and habitat in ceratioid anglerfishes ( $\chi^2 p < 2.2 \times 10^{-16}$ ; Table S1; Figures 2A and 2B).

Handwritten notes:

- They are the sexual parasites
- and facultative parasites
- in Gigantactinidae, Thaumaticichthys, Himantolophus, Oneirodidae, Diceratiidae, and Melanocetus
- Great to see C. bayani stuff here

In contrast, trait-dependent diversification rate analyses using the Binary and Multiple State Speciation and Extinction models (BiSSE and MuSSE)<sup>41</sup> reveal that clades possessing true sexual parasitism and non-parasitic anglerfishes possess similar diversification rates (Figure 2C). Temporarily attaching anglerfish clades show the highest lineage diversification rates (Figures 2A and 2C). Binary trait-based diversification rate analysis shows a clear difference in the diversification rates of benthic and bathypelagic clades (Figure 2B).

Our multistate analysis of habitat-based diversification suggests that shallow-water, predominantly near-shore, and reef-dwelling anglerfishes and the bathypelagic ceratioids have similar diversification rates (Figure 2D). However, bathypelagic anglerfishes have higher diversification rates than benthic deep-water species, which collectively constitute a large proportion of the species diversity of batfishes, goosefishes, and sea toads (Figure 2D). These results suggest that the secondary invasion of the open waters of the deep ocean—the bathypelagic zone—drove the radiation of ceratioid anglerfishes (Figure 2).

### The evolutionary context of reproductive innovation

The genomes of vertebrates encode many receptor families that differentiate normal cells (self) from pathogens and infected cells (non-self). When an endogenous (self) antigen is presented to an immune cell, there is no immune response. In contrast, when a pathogen-derived peptide (non-self) is presented, the immune cell may be engaged and the infected cell destroyed. This presentation of self and non-self antigens in an infected cell is orchestrated by major histocompatibility complex (MHC) molecules in concert with a suite of associated genes and is a key component of vertebrate pathogen defense and immune memory. Yet several species of ray-finned fishes, including seahorses

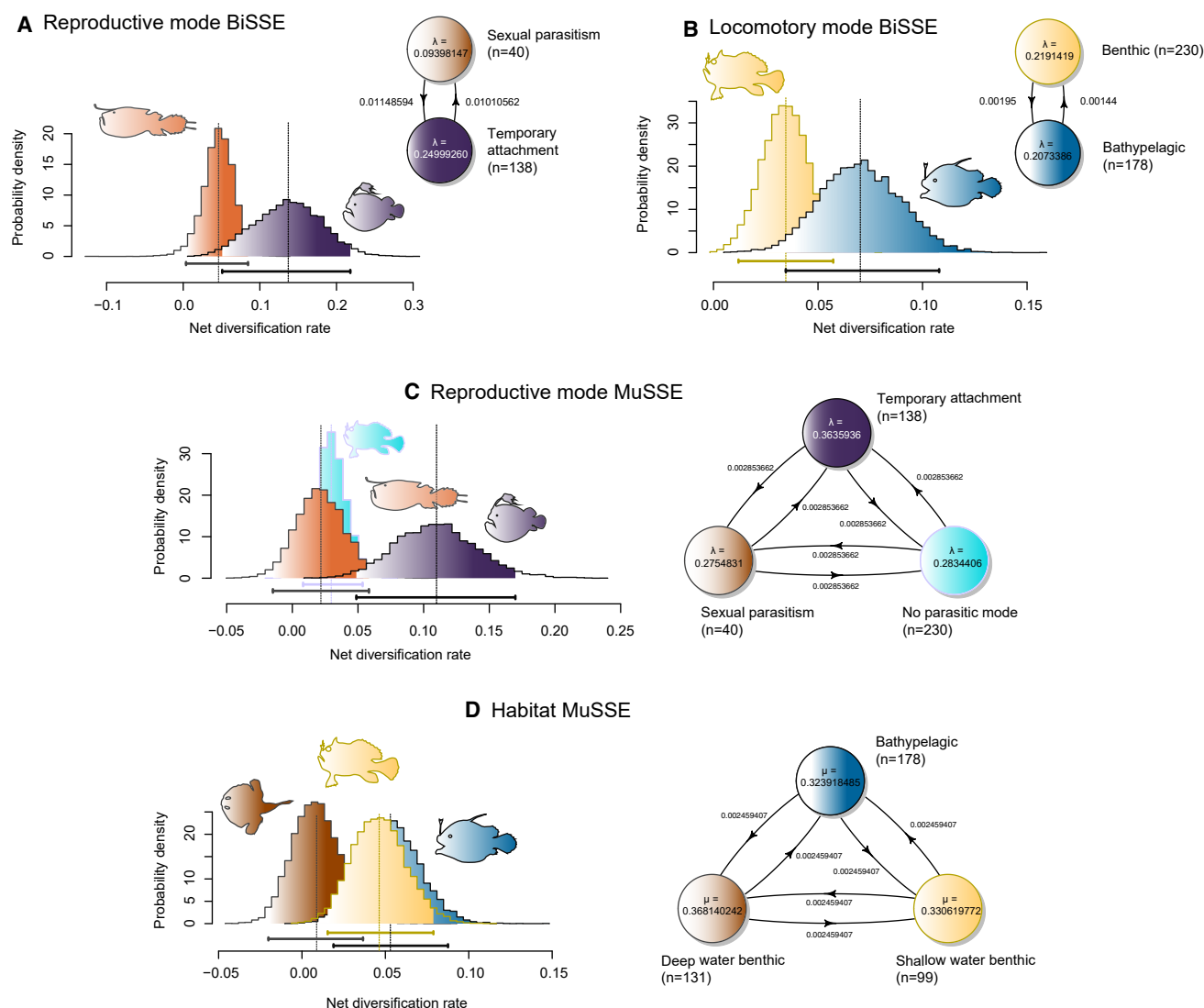


**Figure 2. Ecological and reproductive innovations drove the diversification of anglerfishes**

(A–D) Plots show posterior probability density distributions and transition matrices of net diversification rates in anglerfishes with distinctive ecologies and reproductive modes. (A) and (B) show binary state-dependent diversification rate (BiSSE) runs, and (C) and (D) show multistate-dependent diversification rate (MuSSE) runs for three states. Note that bathypelagic anglerfishes have higher diversification rates than benthic species (B and D), especially compared to deep-sea benthic forms (D). This is driven mainly by diversification associated with the evolution of temporary attachment (A and C). Shaded regions of curves and bars under distribution curves indicate where 95% of the distribution falls. Also see Tables S1 and S2 and Data S3.

and cods, have lost or degenerated the genetic basis of this physiological system.<sup>42–45</sup> In addition to compromising the MHC, sexual parasitism in several lineages of anglerfishes appears to be linked to a degenerated suite of molecular receptors associated with losses to critical aspects of the adaptive immune response such as V(D)J recombination, high-affinity antibody generation, T and B cell development, and antigen display (Figure 3).<sup>11</sup> Collectively, this degeneration of the adaptive immune response is hypothesized to have facilitated the evolution of the reproductive modes of ceratioid anglerfishes.<sup>11</sup> However, the evolution of these modes of sexual parasitism and the corresponding genomic changes has remained unclear.<sup>46</sup> One possibility is that synergistic interactions have occurred between these molecular changes and other key features characterizing

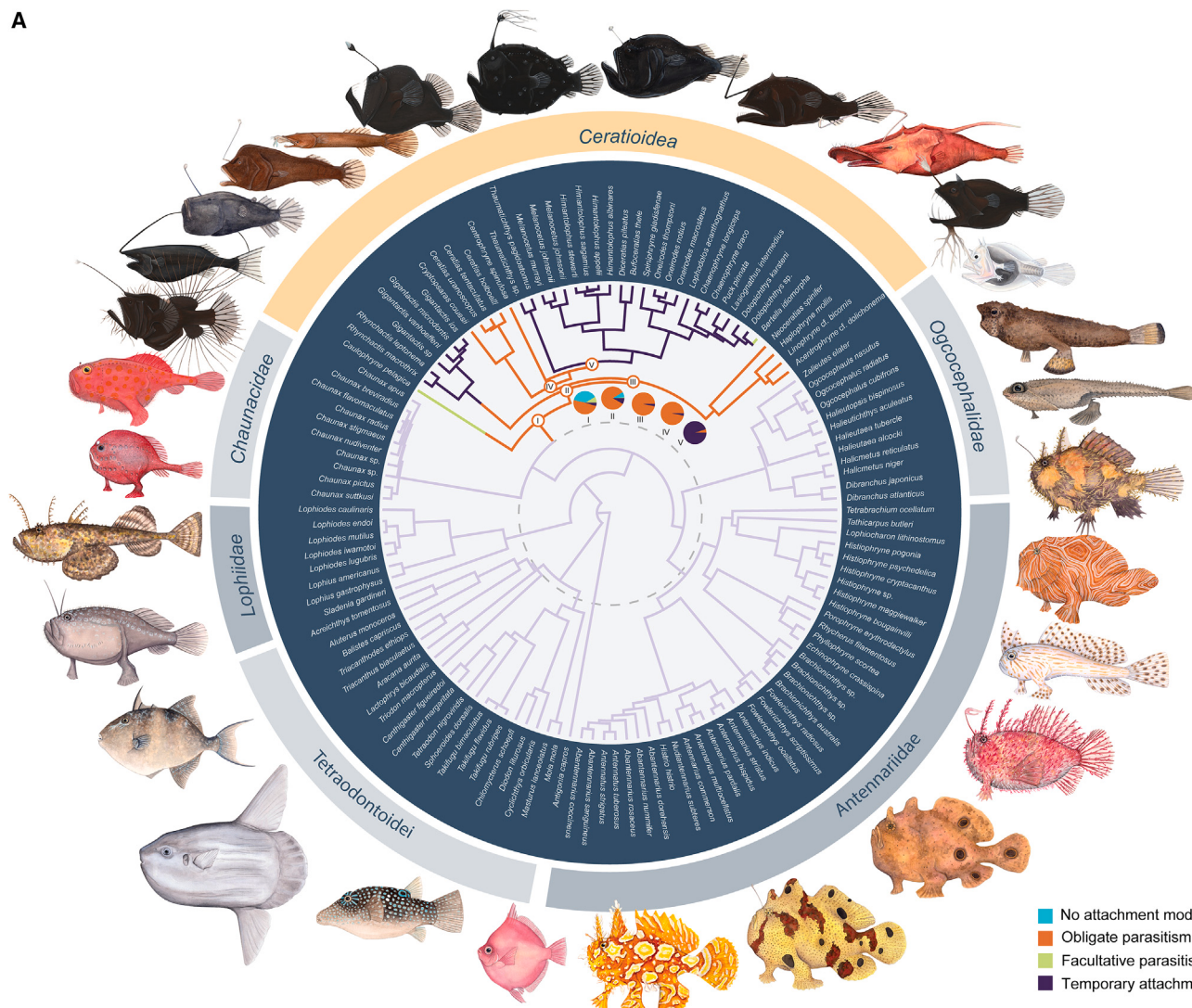
the ceratioid anglerfish radiation, such as extreme sexual dimorphism in body size and a shift in locomotor mode from benthic walking to open-water swimming. Whether these changes occurred during major Cenozoic climate change events, such as the PETM,<sup>14,34,47</sup> is unclear.

The placement of obligate parasites among ceratioid anglerfishes has also remained unresolved over half a century of investigations,<sup>6,10–13,15,25,27</sup> and recent phylogenomic analyses have failed to reach a consensus.<sup>10–12</sup> Our species tree and maximum-likelihood phylogeny do not support the monophyly of obligate parasites, contrasting with recent analyses.<sup>12</sup> Ancestral state reconstructions of reproductive mode on the time-calibrated phylogenies of anglerfishes and tetraodontoids suggest a complex evolutionary history of sexual parasitism. Although

# Current Biology Report

CellPress

A



B

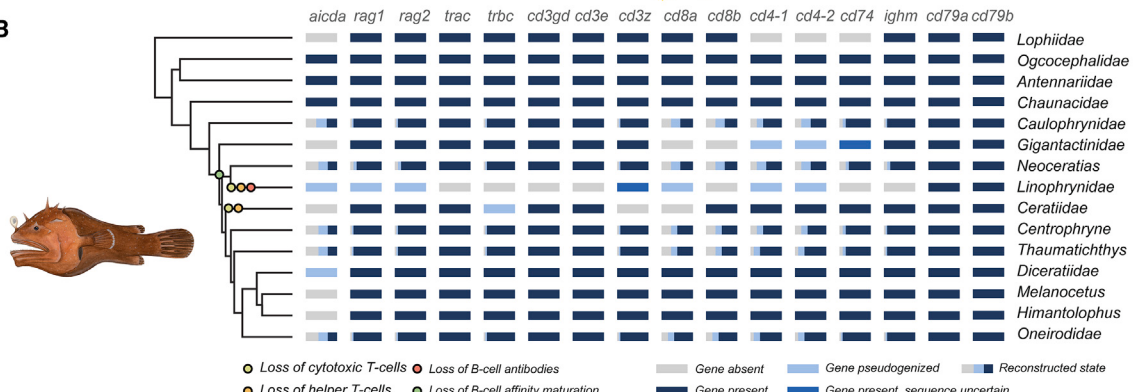


**Figure 3. The evolutionary context of anglerfish immunogenomic degradation**

(A and B) Bayesian timetree in (A) shows an ancestral state reconstruction of reproductive mode in anglerfishes and their sister clade, the *Tetraodontoidei*, based on simulated stochastic character mapping. The dotted line indicates the Cretaceous-Paleogene boundary, and pie charts indicate ancestral state probabilities at key nodes where ancestral states are most uncertain. Light blue indicates no modified reproductive mode, yellow indicates facultative sexual parasitism, orange indicates obligate sexual parasitism, and purple indicates temporary attachment. Time-calibrated phylogeny and table in (B) shows the gene losses and pseudogenizations of key immune genes in anglerfishes based on genomic sequences and simulated stochastic character mapping. Note how different gene losses and pseudogenization events occur in nearly every lineage that displays obligate or facultative sexual parasitism. Also see Data S1. Fish illustrations by Julie Johnson ([www.lifesciencestudios.com](http://www.lifesciencestudios.com)).

obligate parasitism was weakly inferred as the most likely state for the common ancestor of ceratioids, this result is likely driven by the unstable placement of the obligate parasitic lineages in the AZ that covers much of the ceratioid backbone (Figure 3A). However, we do find that at least some mode of sexual parasitism was the ancestral condition for bathypelagic anglerfishes (Figure 3).

Temporary attachment is reconstructed with two origins: once in *Gigantactinidae* and at the MRCA of the clade that includes *Thaumaticichthys*, *Himantolophus*, *Oneirodidae*, *Diceratiidae*, and *Melanocetus* (Figure 3A). All nodes in the AZ are reconstructed as ancestrally sexual parasitic with varying degrees of support (Figures 1 and 3A). The lack of phylogenetic resolution may be the result of incomplete lineage sorting driven by a history of short intervals between divergence events,<sup>17,31,32</sup> suggesting that periods of rapid lineage origination were paired with innovation in reproductive mode in deep-sea anglerfishes.

Recent work has shown that both temporarily attaching and sexually parasitic ceratioid anglerfishes have degenerated the molecular basis of their adaptive immune response.<sup>11</sup> However, different hypotheses of deep-sea anglerfish phylogeny<sup>10–13,25</sup> imply different modes of immunogenomic change. We compiled data on the presence of selected genes relevant to adaptive immunity in anglerfishes from studies of published anglerfish genomes<sup>11,46,48</sup> and then used multiple methods of ancestral state reconstruction to produce gene presence and absence likelihoods for clades lacking sequence data (Figure 3B). Ancestral state reconstructions show that cellular components of adaptive immunity convergently degenerated in clades with parasitic reproductive modes (Figure 3B; Figure S7) rather than via the stepwise loss or pseudogenization of genes along the backbone of the deep-sea anglerfish clade. Further, non-ceratioid lineages such as batfishes and goosefishes demonstrate complex losses and pseudogenizations of key immune genes of non-ceratioid anglerfishes (Figure 3B).

Ogcocephalids, chaunacids, and antennariids show no losses to their adaptive immune genes. However, lophiids have lost virtually all of the genetic basis of the MHC II.<sup>46</sup> These observations, particularly when considered in the context of the various episodes of immunogenomic degeneration in teleost fishes,<sup>45,49</sup> show that key genes involved in adaptive immunity have been variably lost or pseudogenized in lophioids outside of the origins of deep-sea anglerfishes. Similarly, ancestral state reconstructions for sexual body size dimorphism based on recent observations of diminutive males in frogfishes and the deep-sea lophiid *Sladenia gardineri*<sup>50</sup> suggest that significant body size differences between male and female anglerfishes originated prior to the origin of deep-sea ceratioids (Figure S8).

## DISCUSSION

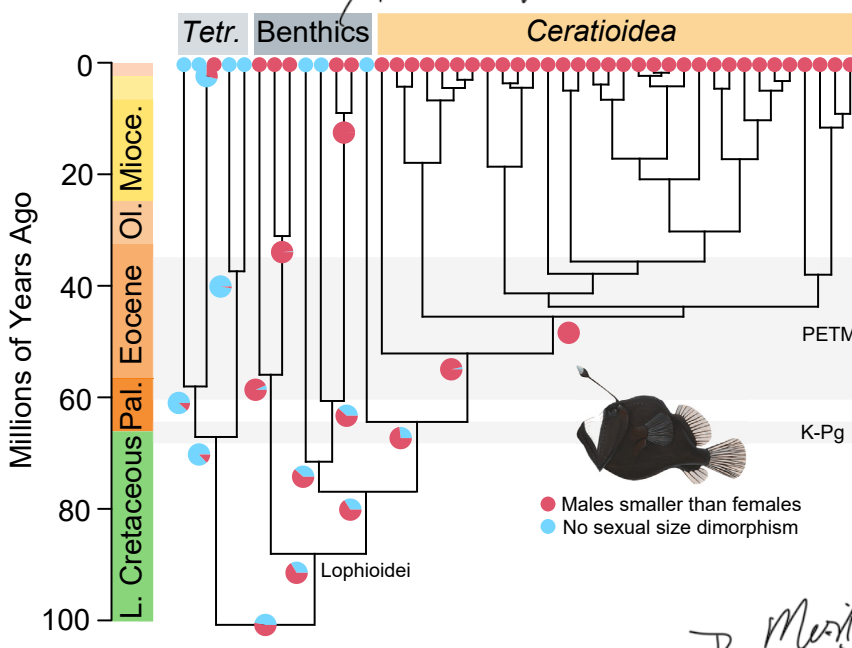
This is very synergistic

Anglerfishes comprise the most species-rich radiation of vertebrates in the deep sea.<sup>7,10,11,13,25,27</sup> This evolutionary feat may have been aided by peculiar reproductive modes that increased the chances of successfully mating in the largest of Earth's ecosystems.<sup>6,7,51</sup> Here, we provide a phylogenomic reconstruction of the evolutionary history of anglerfishes. By examining the evolution of sexual dimorphism and the evolutionary history of genes encoding critical aspects of the adaptive immune response in all major anglerfish lineages using a time-calibrated phylogenomic

tree, we determined that the degeneration of the genomic basis of adaptive immunity and extreme size differences between male and female anglerfishes coincide with the origin of ceratioids and the evolution of sexual parasitism (Figure 3B).<sup>46</sup> Our results suggest that the synergistic interaction of these traits allowed multiple different clades of ceratioid anglerfishes to degenerate their immune systems and develop obligate parasitism (Figure 3B).<sup>11</sup> Collectively, these results suggest that the development of new modes of reproduction in deep-sea anglerfishes was a synergistic process involving the loss of core immunogenetic functionality and extreme sexual size dimorphism (Figure 3). However, it was the confluence of this complex trait with a major ecological transition into the open ocean during a period of intense global ecological stress that facilitated higher rates of diversification in bathypelagic lineages.

Our results implicate the degradation of the genetic basis of adaptive immunity and extreme sexual dimorphism as mechanisms driving the ecological transition of ceratioid anglerfishes into deep-sea open-water habitats. Several genes involved in vertebrate adaptive immunity, among them *aicda*, which is involved in B-lymphocyte development, were lost prior to the MRCA of *Ceratioidea*, potentially compromising the ability to generate high-affinity antibodies or switch between antibody isotopes (IgT, IgM, etc.<sup>52</sup>; Figure 3B) in anglerfishes. This timing is coincident with a dramatic shift toward extreme size dimorphism between male and female ceratioid anglerfishes (Figure 4). Puth, Diminutive males of non-ceratioid anglerfishes are known to closely follow the larger females,<sup>50</sup> suggesting that behaviors reminiscent of temporary attachment are much more widespread within *Lophioidei*. In lineages such as the obligate sexual parasites *Linophrynidae*, the lack of a functional antibody response likely set the stage for a suite of losses otherwise critical for the adaptive immune response including V(D)J recombination mediated by *rag1* and *rag2*, MHCII antigen display with *cd74*, and T cell functionality that now enables fusion of male anglerfish to females. Together with ancestral state reconstructions (Figure 4; Figure S8), these observations indicate that sexual parasitism was assembled from a suite of genomic, morphological, and behavioral characteristics with evolutionary origins stretching back into the Late Cretaceous (Figures 1 and 3).

There is a quantifiably unstable phylogenomic backbone that corresponds to the initial diversification of ceratioid anglerfishes (Figure 1; Figures S4 and S5), which radiated in open water habitats after evolving from benthic fin-walking ancestors (Figures 1 and 2B). Such phylogenetic uncertainty might be expected if anglerfishes radiated during or just after a major extinction or turnover event, such as the biotic crisis associated with the PETM. The extensive gene tree discordance and short branch lengths across the ceratioid phylogenomic backbone are indicative of ancestral polymorphism resulting from variables such as large ancestral effective population sizes and relatively short intervals between speciation events<sup>17,31,32</sup> (Figures 1, 2B, and 2D). Rather than resulting from methodological or sampling artifacts, the AZ at the base of ceratioids appears to reflect their ancient evolutionary history. Similarly discordant nodes have been found in clades like birds that underwent adaptive radiation following major extinction events.<sup>53–56</sup> The time-calibrated phylogeny generated in this study shows that nearly all ceratioid lineages classified as taxonomic families appeared during the PETM (Figure 1), an interval marked



by major marine turnovers and extinction events, including lineages of the *Tetraodontoidae*, the sister clade to anglerfishes.<sup>34</sup>

Nearly all examples of evolutionary radiations highlight single traits that are held responsible for directly promoting specialization in new ecological niches. Classic examples include the fused pharyngeal jaws of cichlid fishes<sup>57–62</sup> and the beaks of Darwin's Finches.<sup>63–65</sup> Our results suggest that extreme sexual size dimorphism and loss of the adaptive immune response form the synovation that gave rise to sexual parasitism, a trait that facilitated access to a previously inaccessible ecosystem by ensuring reproductive success.<sup>1,4</sup> This result explains how this novel reproductive strategy suddenly appeared in ceratioids. However, examination of trait-dependent diversification rates suggests that ceratioid diversification<sup>39</sup> is best explained by a combination of reproductive mode innovation and the ecological opportunities available in the bathypelagic zone (Figure 2) during the PETM (Figure 1) rather than solely by their unusual reproductive strategies. A complex evolutionary cascade of many different traits, including sexual dimorphism, degeneration of many key pathways of the adaptive immune system, and the evolution of a body plan suited for a pelagic lifestyle, facilitated anglerfish diversification in the bathypelagic zone as oceanic ecosystems faced extreme global warming. In this way, the sexual parasitism of ceratioid anglerfishes provides an apt example of key innovation as the term was originally conceived<sup>1,66,67</sup> and shows how these traits need not be solely responsible for the evolutionary diversification of a lineage.

## STAR METHODS

Detailed methods are provided in the online version of this paper and include the following:

- KEY RESOURCES TABLE
- RESOURCE AVAILABILITY
  - Lead contact
  - Materials availability
  - Data and code availability

- EXPERIMENTAL MODEL AND SUBJECT DETAILS
- METHOD DETAILS
  - Taxon sampling and sequencing methods
  - UCE sequence alignment, sanitation, and preprocessing
  - Maximum likelihood phylogenetic analyses
  - Concordance factors and anomaly zone detection
  - Divergence time estimation
  - Ancestral state reconstructions
  - Chaunacid mitochondrial gene tree and genetic distances
  - Trait-based species richness and diversification rates
  - Evolutionary history of anglerfish immunogenetics
- QUANTIFICATION AND STATISTICAL ANALYSIS

## SUPPLEMENTAL INFORMATION

Supplemental information can be found online at <https://doi.org/10.1016/j.cub.2024.04.066>.

## ACKNOWLEDGMENTS

We thank members of the Near and Dornburg labs for discussions regarding ray-finned fish and anglerfish evolution. For critical tissues we thank T. Sutton, A. Cook, A. Bernard, H. Bracken-Grissom, M. Shivji, J. Moore, Wei-Jen Chen, and Carl Struthers. This work was supported by the National Science Foundation (IOS1755242 to A.D.) and the Bingham Oceanographic Fund maintained by the Peabody Museum, Yale University.

## AUTHOR CONTRIBUTIONS

C.D.B., K.L.Z., S.L., R.H., A.G., A.D., and T.J.N. collected and processed the data, and C.D.B., K.L.Z., S.L., and A.D. conducted analyses. C.D.B. wrote the paper with input from the other authors.

## DECLARATION OF INTERESTS

The authors declare no competing interests.

Received: January 9, 2024

Revised: March 10, 2024

Accepted: April 29, 2024

Published: May 23, 2024

REFERENCES

1. Miller, A.H., Stroud, J.T., and Losos, J.B. (2023). The ecology and evolution of key innovations. *Trends Ecol. Evol.* 38, 122–131. <https://doi.org/10.1016/j.tree.2022.09.005>.
2. Stroud, J.T., and Losos, J.B. (2016). Ecological Opportunity and Adaptive Radiation. *Annu. Rev. Ecol. Syst.* 47, 507–532. <https://doi.org/10.1146/annurev-ecolsys-121415-032254>.
3. Gavrilets, S., and Losos, J.B. (2009). Adaptive Radiation: Contrasting Theory with Data. *Science* 323, 732–737. <https://doi.org/10.1126/science.1157966>.
4. Donoghue, M.J., and Sanderson, M.J. (2015). Confluence, synnovation, and depauperons in plant diversification. *New Phytol.* 207, 260–274. <https://doi.org/10.1111/nph.13367>.
5. Pietsch, T.W. (2009). *Oceanic Anglerfishes: Extraordinary Diversity in the Deep Sea*, 1st ed. (University of California Press).
6. Pietsch, T.W. (1976). Dimorphism, Parasitism and Sex: Reproductive Strategies among Deepsea Ceratioid Anglerfishes. *Copeia* 1976, 781–793. <https://doi.org/10.2307/1443462>.
7. Pietsch, T.W. (2005). Dimorphism, parasitism, and sex revisited: modes of reproduction among deep-sea ceratioid anglerfishes (Teleostei: Lophiiformes). *Ichthyol. Res.* 52, 207–236. <https://doi.org/10.1007/s10228-005-0286-2>.
8. Westerhold, T., Marwan, N., Drury, A.J., Liebrand, D., Agnini, C., Anagnostou, E., Barnet, J.S.K., Bohaty, S.M., De Vleeschouwer, D., Florindo, F., et al. (2020). An astronomically dated record of Earth's climate and its predictability over the last 66 million years. *Science* 369, 1383–1387. <https://doi.org/10.1126/science.aba6853>.
9. Meckler, A.N., Sexton, P.F., Piasecki, A.M., Leutert, T.J., Marquardt, J., Ziegler, M., Agterhuis, T., Lourens, L.J., Rae, J.W.B., Barnet, J., et al. (2022). Cenozoic evolution of deep ocean temperature from clumped isotope thermometry. *Science* 377, 86–90. <https://doi.org/10.1126/science.abk0604>.
10. Hart, P.B., Arnold, R.J., Alda, F., Kenaley, C.P., Pietsch, T.W., Hutchinson, D., and Chakrabarty, P. (2022). Evolutionary relationships of anglerfishes (Lophiiformes) reconstructed using ultraconserved elements. *Mol. Phylogenetic Evol.* 171, 107459. <https://doi.org/10.1016/j.ympev.2022.107459>.
11. Swann, J.B., Holland, S.J., Petersen, M., Pietsch, T.W., and Boehm, T. (2020). The immunogenetics of sexual parasitism. *Science* 369, 1608–1615. <https://doi.org/10.1126/science.aaz9445>.
12. Ghezelayagh, A., Harrington, R.C., Burress, E.D., Campbell, M.A., Buckner, J.C., Chakrabarty, P., Glass, J.R., McCraney, W.T., Unmack, P.J., Thacker, C.E., et al. (2022). Prolonged morphological expansion of spiny-rayed fishes following the end-Cretaceous. *Nat. Ecol. Evol.* 6, 1211–1220. <https://doi.org/10.1038/s41559-022-01801-3>.
13. Miya, M., Pietsch, T.W., Orr, J.W., Arnold, R.J., Satoh, T.P., Shedlock, A.M., Ho, H.-C., Shimazaki, M., Yabe, M., and Nishida, M. (2010). Evolutionary history of anglerfishes (Teleostei: Lophiiformes): a mitogenomic perspective. *BMC Evol. Biol.* 10, 58. <https://doi.org/10.1186/1471-2148-10-58>.
14. Troyer, E.M., Betancur-R, R., Hughes, L.C., Westneat, M., Carnevale, G., White, W.T., Pogonoski, J.J., Tyler, J.C., Baldwin, C.C., Ortí, G., et al. (2022). The impact of paleoclimatic changes on body size evolution in marine fishes. *pnas* 119, pp. e2122486119. <https://doi.org/10.1073/pnas.2122486119>.
15. Near, T.J., Dornburg, A., Eytan, R.I., Keck, B.P., Smith, W.L., Kuhn, K.L., Moore, J.A., Price, S.A., Burbink, F.T., Friedman, M., and Wainwright, P.C. (2013). Phylogeny and tempo of diversification in the superradiation of spiny-rayed fishes. *pnas* 110, pp. 12738–12743. <https://doi.org/10.1073/pnas.1304661110>.
16. Faircloth, B.C. (2016). PHYLUCE is a software package for the analysis of conserved genomic loci. *Bioinformatics* 32, 786–788. <https://doi.org/10.1093/bioinformatics/btv646>.
17. Degnan, J.H., and Rosenberg, N.A. (2006). Discordance of Species Trees with Their Most Likely Gene Trees. *PLoS Genet.* 2, e68. <https://doi.org/10.1371/journal.pgen.0020068>.
18. Tumescheit, C., Firth, A.E., and Brown, K. (2022). ClAlign: A highly customisable command line tool to clean, interpret and visualise multiple sequence alignments. *PeerJ* 10, e12983. <https://doi.org/10.7717/peerj.12983>.
19. Minh, B.Q., Schmidt, H.A., Chernomor, O., Schrempf, D., Woodhams, M.D., von Haeseler, A., and Lanfear, R. (2020). IQ-TREE 2: New Models and Efficient Methods for Phylogenetic Inference in the Genomic Era. *Mol. Biol. Evol.* 37, 1530–1534. <https://doi.org/10.1093/molbev/msaa015>.
20. Nguyen, L.-T., Schmidt, H.A., von Haeseler, A., and Minh, B.Q. (2015). IQ-TREE: A Fast and Effective Stochastic Algorithm for Estimating Maximum-Likelihood Phylogenies. *Mol. Biol. Evol.* 32, 268–274. <https://doi.org/10.1093/molbev/msu300>.
21. Wcislo, D.J., Howard, J.T., Yoder, J.A., and Dornburg, A. (2020). Transcriptome Ortholog Alignment Sequence Tools (TOAST) for phylogenomic dataset assembly. *BMC Evol. Biol.* 20, 41. <https://doi.org/10.1186/s12862-020-01603-w>.
22. Naser-Khdour, S., Minh, B.Q., Zhang, W., Stone, E.A., and Lanfear, R. (2019). The Prevalence and Impact of Model Violations in Phylogenetic Analysis. *Genome Biol. Evol.* 11, 3341–3352. <https://doi.org/10.1093/gbe/evz193>.
23. Zhang, C., Rabiee, M., Sayyari, E., and Mirarab, S. (2018). ASTRAL-III: polynomial time species tree reconstruction from partially resolved gene trees. *BMC Bioinf.* 19, 153. <https://doi.org/10.1186/s12859-018-2129-y>.
24. Dickson, B.V., and Pierce, S.E. (2018). How (and why) fins turn into limbs: insights from anglerfish. *Earth and Environmental Science Transactions of The Royal Society of Edinburgh* 109, 87–103. <https://doi.org/10.1017/S1755691018000415>.
25. Shedlock, A.M., Pietsch, T.W., Haygood, M.G., Bentzen, P., Hasegawa, M. (2004). Molecular systematics and life history evolution of anglerfishes (Teleostei: Lophiiformes): Evidence from mitochondrial DNA. *Steenstrupia* 28:129–144. [https://www.researchgate.net/publication/229003577\\_Molecular\\_systematics\\_and\\_life\\_history\\_evolution\\_of\\_anglerfishes\\_Teleostei\\_Lophiiformes\\_Evidence\\_from\\_mitochondrial\\_DNA](https://www.researchgate.net/publication/229003577_Molecular_systematics_and_life_history_evolution_of_anglerfishes_Teleostei_Lophiiformes_Evidence_from_mitochondrial_DNA).
26. Betancur-R, R., Wiley, E.O., Arratia, G., Acero, A., Bailly, N., Miya, M., Lecointre, G., and Ortí, G. (2017). Phylogenetic classification of bony fishes. *BMC Evol. Biol.* 17, 162. <https://doi.org/10.1186/s12862-017-0958-3>.
27. Pietsch, T.W., and Orr, J.W. (2007). Phylogenetic Relationships of Deep-sea Anglerfishes of the Suborder Ceratioidei (Teleostei: Lophiiformes) Based on Morphology. *COPE* 2007, 1–34. [https://doi.org/10.1643/0045-8511\(2007\)7\[1:PRODAO\]2.0.CO;2](https://doi.org/10.1643/0045-8511(2007)7[1:PRODAO]2.0.CO;2).
28. Uhen, M.D. (2010). The Origin(s) of Whales. *Annu. Rev. Earth Planet Sci.* 38, 189–219. <https://doi.org/10.1146/annurev-earth-040809-152453>.
29. Gingerich, P.D. (2003). Land-to-sea transition in early whales: evolution of Eocene Archaeoceti (Cetacea) in relation to skeletal proportions and locomotion of living semiaquatic mammals. *Paleobiology* 29, 429–454. [https://doi.org/10.1666/0094-8373\(2003\)029<429:LTS>2.0.CO;2](https://doi.org/10.1666/0094-8373(2003)029<429:LTS>2.0.CO;2).
30. Motani, R., Jiang, D.-Y., Chen, G.-B., Tintori, A., Rieppel, O., Ji, C., and Huang, J.-D. (2015). A basal ichthyosauriform with a short snout from the Lower Triassic of China. *Nature* 517, 485–488. <https://doi.org/10.1038/nature13866>.
31. Chafin, T.K., Douglas, M.R., Bangs, M.R., Martin, B.T., Mussmann, S.M., and Douglas, M.E. (2021). Taxonomic Uncertainty and the Anomaly Zone: Phylogenomics Disentangle a Rapid Radiation to Resolve Contentious Species (Gila robusta Complex) in the Colorado River. *Genome Biol. Evol.* 13, evab200. <https://doi.org/10.1093/gbe/evab200>.
32. Linkem, C.W., Minin, V.N., and Leaché, A.D. (2016). Detecting the Anomaly Zone in Species Trees and Evidence for a Misleading Signal in Higher-Level Skink Phylogeny (Squamata: Scincidae). *Syst. Biol.* 65, 465–477. <https://doi.org/10.1093/sysbio/syw001>.

# Current Biology Report



33. Bouckaert, R., Heled, J., Kühnert, D., Vaughan, T., Wu, C.-H., Xie, D., Suchard, M.A., Rambaut, A., and Drummond, A.J. (2014). BEAST 2: A Software Platform for Bayesian Evolutionary Analysis. *PLoS Comput. Biol.* 10, e1003537. <https://doi.org/10.1371/journal.pcbi.1003537>.
34. Arcila, D., and Tyler, J.C. (2017). Mass extinction in tetraodontiform fishes linked to the Palaeocene–Eocene thermal maximum. *Proc. Biol. Sci.* 284, 20171771. <https://doi.org/10.1098/rspb.2017.1771>.
35. Sibert, E.C., Hull, P.M., and Norris, R.D. (2014). Resilience of Pacific pelagic fish across the Cretaceous/Palaeogene mass extinction. *Nat. Geosci.* 7, 667–670. <https://doi.org/10.1038/ngeo2227>.
36. Ivany, L.C., Pietsch, C., Handley, J.C., Lockwood, R., Allmon, W.D., and Sessa, J.A. (2018). Little lasting impact of the Paleocene-Eocene Thermal Maximum on shallow marine molluscan faunas. *Sci. Adv.* 4, eaat5528. <https://doi.org/10.1126/sciadv.aat5528>.
37. Westerhold, T., Röhl, U., Donner, B., and Zachos, J.C. (2018). Global Extent of Early Eocene Hyperthermal Events: A New Pacific Benthic Foraminiferal Isotope Record From Shatsky Rise (ODP Site 1209). *Paleoceanogr. Paleoceanogr.* 33, 626–642. <https://doi.org/10.1029/2017PA003306>.
38. Arcila, D., Alexander Pyron, R., Tyler, J.C., Ortí, G., and Betancur-R, R. (2015). An evaluation of fossil tip-dating versus node-age calibrations in tetraodontiform fishes (Teleostei: Percomorphaceae). *Mol. Phylogenet. Evol.* 82, 131–145. <https://doi.org/10.1016/j.ympev.2014.10.011>.
39. Heiple, Z., Huie, J.M., Medeiros, A.P.M., Hart, P.B., Goatley, C.H.R., Arcila, D., and Miller, E.C. (2023). Many ways to build an angler: diversity of feeding morphologies in a deep-sea evolutionary radiation. *Biol. Lett.* 19, 20230049. <https://doi.org/10.1098/rsbl.2023.0049>.
40. Tate Regan, C. (1930). Angler-Fishes. *Nature* 125, 747–749. <https://doi.org/10.1038/125747a0>.
41. FitzJohn, R.G. (2012). Diversitree : comparative phylogenetic analyses of diversification in R: *Diversitree*. *Methods Ecol. Evol.* 3, 1084–1092. <https://doi.org/10.1111/j.2041-210X.2012.00234.x>.
42. Haase, D., Roth, O., Kalbe, M., Schmiedeskamp, G., Scharsack, J.P., Rosenstiel, P., and Reusch, T.B.H. (2013). Absence of major histocompatibility complex class II mediated immunity in pipefish, *Syngnathus typhle*: evidence from deep transcriptome sequencing. *Biol. Lett.* 9, 20130044. <https://doi.org/10.1098/rsbl.2013.0044>.
43. Roth, O., Solbakken, M.H., Tørresen, O.K., Bayer, T., Matschiner, M., Baalsrud, H.T., Hoff, S.N.K., Brieuc, M.S.O., Haase, D., Hamel, R., et al. (2020). Evolution of male pregnancy associated with remodeling of canonical vertebrate immunity in seahorses and pipefishes. *Nature* 577, pp. 9431–9439. <https://doi.org/10.1073/pnas.1916251117>.
44. Liu, Y., Qu, M., Jiang, H., Schneider, R., Qin, G., Luo, W., Yu, H., Zhang, B., Wang, X., Zhang, Y., et al. (2022). Immunogenetic losses co-occurred with seahorse male pregnancy and mutation in *tlx1* accompanied functional asplenia. *Nat. Commun.* 13, 7610. <https://doi.org/10.1038/s41467-022-35338-7>.
45. Star, B., Nederbragt, A.J., Jentoft, S., Grimholt, U., Malmström, M., Gregers, T.F., Rounge, T.B., Paulsen, J., Solbakken, M.H., Sharma, A., et al. (2011). The genome sequence of Atlantic cod reveals a unique immune system. *Nature* 477, 207–210. <https://doi.org/10.1038/nature10342>.
46. Dubin, A., Jørgensen, T.E., Mour, T., Johansen, S.D., and Jakt, L.M. (2019). Complete loss of the MHC II pathway in an anglerfish, *Lophius piscatorius*. *Biol. Lett.* 15, 20190594. <https://doi.org/10.1098/rsbl.2019.0594>.
47. Sibert, E.C., Zill, M.E., Frigyk, E.T., and Norris, R.D. (2020). No state change in pelagic fish production and biodiversity during the Eocene–Oligocene transition. *Nat. Geosci.* 13, 238–242. <https://doi.org/10.1038/s41561-020-0540-2>.
48. Swann, J.B., Grammer, C., Schorpp, M., and Boehm, T. (2023). A survey of the adaptive immune genes of the polka-dot batfish *Ogocephalus cubifrons*. *BMC Immunol.* 24, 20. <https://doi.org/10.1186/s12865-023-00557-0>.
49. Parker, J., Dubin, A., and Roth, O. (2023). Genome rearrangements, male pregnancy and immunological tolerance – the curious case of the syngnathid immune system. *Front. Mar. Sci.* 10.
50. Pietsch, T.W., Ross, S.W., Caruso, J.H., Saunders, M.G., and Fisher, C.R. (2013). In-Situ Observations of the Deep-sea Goosefish *Sladenia shaefersi* Caruso and Bullis (Lophiiformes: Lophiidae), with Evidence of Extreme Sexual Dimorphism. *COPE* 2013, 660–665. <https://doi.org/10.1643/CI-13-023>.
51. Vieira, S., Biscoito, M., Encarnação, H., Delgado, J., and Pietsch, T.W. (2013). Sexual Parasitism in the Deep-sea Ceratioid Anglerfish *Centroprhyne spinulosa* Regan and Trewavas (Lophiiformes: Centroprynidae). *Copeia* 2013, 666–669. <https://doi.org/10.1643/CI-13-035>.
52. Dornburg, A., Ota, T., Criscitiello, M.F., Salinas, I., Sunyer, J.O., Magadán, S., Boudinot, P., Xu, Z., Flajnik, M.F., Singer, A., et al. (2021). From IgZ to IgT: A Call for a Common Nomenclature for Immunoglobulin Heavy Chain Genes of Ray-Finned Fish. *Zebrafish* 18, 343–345. <https://doi.org/10.1089/zeb.2021.0071>.
53. Jarvis, E.D., Mirarab, S., Aberer, A.J., Li, B., Houde, P., Li, C., Ho, S.Y.W., Faircloth, B.C., Nabholz, B., Howard, J.T., et al. (2014). Whole-genome analyses resolve early branches in the tree of life of modern birds. *Science* 346, 1320–1331. <https://doi.org/10.1126/science.1253451>.
54. Prum, R.O., Berv, J.S., Dornburg, A., Field, D.J., Townsend, J.P., Lemmon, E.M., and Lemmon, A.R. (2015). A comprehensive phylogeny of birds (Aves) using targeted next-generation DNA sequencing. *Nature* 526, 569–573. <https://doi.org/10.1038/nature15697>.
55. Reddy, S., Kimball, R.T., Pandey, A., Hosner, P.A., Braun, M.J., Hackett, S.J., Han, K.-L., Harshman, J., Huddleston, C.J., Kingston, S., et al. (2017). Why Do Phylogenomic Data Sets Yield Conflicting Trees? Data Type Influences the Avian Tree of Life more than Taxon Sampling. *Syst. Biol.* 66, 857–879. <https://doi.org/10.1093/sysbio/syx041>.
56. Kuhl, H., Frankl-Vilches, C., Bakker, A., Mayr, G., Nikolaus, G., Boerno, S.T., Klages, S., Timmermann, B., and Gahr, M. (2021). An Unbiased Molecular Approach Using 3'-UTRs Resolves the Avian Family-Level Tree of Life. *Mol. Biol. Evol.* 38, 108–127. <https://doi.org/10.1093/molbev/msaa191>.
57. Burress, E.D. (2016). Ecological diversification associated with the pharyngeal jaw diversity of Neotropical cichlid fishes. *J. Anim. Ecol.* 85, 302–313. <https://doi.org/10.1111/1365-2656.12457>.
58. Conith, A.J., and Albertson, R.C. (2021). The cichlid oral and pharyngeal jaws are evolutionarily and genetically coupled. *Nat. Commun.* 12, 5477. <https://doi.org/10.1038/s41467-021-25755-5>.
59. Liem, K.F. (1973). Evolutionary Strategies and Morphological Innovations: Cichlid Pharyngeal Jaws. *Syst. Zool.* 22, 425–441. <https://doi.org/10.2307/2412950>.
60. McGee, M.D., Borstein, S.R., Neches, R.Y., Buescher, H.H., Seehausen, O., and Wainwright, P.C. (2015). A pharyngeal jaw evolutionary innovation facilitated extinction in Lake Victoria cichlids. *Science* 350, 1077–1079. <https://doi.org/10.1126/science.aab0800>.
61. Ronco, F., and Salzburger, W. (2021). Tracing evolutionary decoupling of oral and pharyngeal jaws in cichlid fishes. *Evol. Lett.* 5, 625–635. <https://doi.org/10.1002/evl3.257>.
62. Darrin Hulsey, C. (2006). Function of a key morphological innovation: fusion of the cichlid pharyngeal jaw. *Proc. Biol. Sci.* 273, 669–675. <https://doi.org/10.1098/rspb.2005.3375>.
63. Abzhanov, A., Protas, M., Grant, B.R., Grant, P.R., and Tabin, C.J. (2004). Bmp4 and Morphological Variation of Beaks in Darwin's Finches. *Science* 305, 1462–1465. <https://doi.org/10.1126/science.1098095>.
64. Lamichhaney, S., Berglund, J., Almén, M.S., Maqbool, K., Grabherr, M., Martinez-Barrio, A., Promerová, M., Rubin, C.-J., Wang, C., Zamani, N., et al. (2015). Evolution of Darwin's finches and their beaks revealed by genome sequencing. *Nature* 518, 371–375. <https://doi.org/10.1038/nature14181>.

65. Grant, P.R., and Grant, B.R. (2006). Evolution of Character Displacement in Darwin's Finches. *Science* 313, 224–226. <https://doi.org/10.1126/science.1128374>.
66. Van Valen, L. (1971). Adaptive Zones and the Orders of Mammals. *Evolution* 25, 420–428. <https://doi.org/10.2307/2406935>.
67. Simpson, G.G. (1953). *The major features of evolution* (New York: Columbia University Press).
68. Bouckaert, R., Vaughan, T.G., Barido-Sottani, J., Duchêne, S., Fourment, M., Gavryushkina, A., Heled, J., Jones, G., Kühnert, D., De Maio, N., et al. (2019). BEAST 2.5: An advanced software platform for Bayesian evolutionary analysis. *PLoS Comput. Biol.* 15, e1006650. <https://doi.org/10.1371/journal.pcbi.1006650>.
69. Revell, L.J. (2012). phytools: an R package for phylogenetic comparative biology (and other things). *Methods Ecol. Evol.* 3, 217–223. <https://doi.org/10.1111/j.2041-210X.2011.00169.x>.
70. Rambaut, A., Drummond, A.J., Xie, D., Baele, G., and Suchard, M.A. (2018). Posterior Summarization in Bayesian Phylogenetics Using Tracer 1.7. *Syst. Biol.* 67, 901–904. <https://doi.org/10.1093/sysbio/syy032>.
71. Kalyaanamoorthy, S., Minh, B.Q., Wong, T.K.F., von Haeseler, A., and Jermiin, L.S. (2017). ModelFinder: fast model selection for accurate phylogenetic estimates. *Nat. Methods* 14, 587–589. <https://doi.org/10.1038/nmeth.4285>.
72. Alfaro, M.E., Faircloth, B.C., Harrington, R.C., Sorenson, L., Friedman, M., Thacker, C.E., Oliveros, C.H., Černý, D., and Near, T.J. (2018). Explosive diversification of marine fishes at the Cretaceous–Palaeogene boundary. *Nat. Ecol. Evol.* 2, 688–696. <https://doi.org/10.1038/s41559-018-0494-6>.
73. Carnevale, G., and Pietsch, T.W. (2010). Eocene handfishes from Monte Bolca, with description of a new genus and species, and a phylogeny of the family Brachionichthyidae (Teleostei: Lophiiformes). *Zool. J. Linn. Soc.* 160, 621–647. <https://doi.org/10.1111/j.1096-3642.2009.00623.x>.
74. Pietsch, T.W., and Grobecker, D.B. (1987). *Frogfishes of the World: Systematics, Zoogeography, and Behavioral Ecology* (Stanford University Press).
75. Near, T.J., and Thacker, C.E. (2024). Phylogenetic classification of living and fossil ray-finned fishes (Actinopterygii). *Bull. - Peabody Mus. Nat. Hist.* 65, <https://doi.org/10.5281/zenodo.8352027>.
76. Faircloth, B.C., Sorenson, L., Santini, F., and Alfaro, M.E. (2013). A Phylogenomic Perspective on the Radiation of Ray-Finned Fishes Based upon Targeted Sequencing of Ultraconserved Elements (UCEs). *PLoS One* 8, e65923. <https://doi.org/10.1371/journal.pone.0065923>.
77. Glenn, T.C., Nilsen, R.A., Kieran, T.J., Sanders, J.G., Bayona-Vásquez, N.J., Finger, J.W., Pierson, T.W., Bentley, K.E., Hoffberg, S.L., Louha, S., et al. (2019). Adapterama I: universal stubs and primers for 384 unique dual-indexed or 147,456 combinatorially-indexed Illumina libraries (iTru & iNext). *PeerJ* 7, e7755. <https://doi.org/10.7717/peerj.7755>.
78. Thines, M., Aoki, T., Crouse, P.W., Hyde, K.D., Lücking, R., Malosso, E., May, T.W., Miller, A.N., Redhead, S.A., Yurkov, A.M., et al. (2020). Setting scientific names at all taxonomic ranks in italics facilitates their quick recognition in scientific papers. *IMA Fungus* 11, 25. <https://doi.org/10.1186/s43008-020-00048-6>.
79. Hoang, D.T., Chernomor, O., von Haeseler, A., Minh, B.Q., and Vinh, L.S. (2018). UFBoot2: Improving the Ultrafast Bootstrap Approximation. *Mol. Biol. Evol.* 35, 518–522. <https://doi.org/10.1093/molbev/msx281>.
80. Lanfear, R., Frandsen, P.B., Wright, A.M., Senfeld, T., and Calcott, B. (2017). PartitionFinder 2: New Methods for Selecting Partitioned Models of Evolution for Molecular and Morphological Phylogenetic Analyses. *Mol. Biol. Evol.* 34, 772–773. <https://doi.org/10.1093/molbev/msw260>.
81. Gavryushkina, A., Heath, T.A., Ksepka, D.T., Stadler, T., Welch, D., and Drummond, A.J. (2017). Bayesian Total-Evidence Dating Reveals the Recent Crown Radiation of Penguins. *Syst. Biol.* 66, 57–73. <https://doi.org/10.1093/sysbio/syw060>.
82. Brownstein, C.D. (2023). Syngnathoid Evolutionary History and the Conundrum of Fossil Misplacement. *Integr. Org. Biol.* 5, obad011. <https://doi.org/10.1093/iob/obad011>.
83. Friedman, M., Andrews, J.V., Saad, H., and El-Sayed, S. (2023). The Cretaceous–Paleogene transition in spiny-rayed fishes: surveying “Patterson’s Gap” in the acanthomorph skeletal record André Dumont medalist lecture 2018. *Geol. Belg.* 26, 1–23. <https://doi.org/10.20341/gb.2023.002>.
84. Near, T.J., Eytan, R.I., Dornburg, A., Kuhn, K.L., Moore, J.A., Davis, M.P., Wainwright, P.C., Friedman, M., and Smith, W.L. (2012). Resolution of ray-finned fish phylogeny and timing of diversification 109, pp. 13698–13703. <https://doi.org/10.1073/pnas.1206625109>.
85. Hughes, L.C., Ortí, G., Huang, Y., Sun, Y., Baldwin, C.C., Thompson, A.W., Arcila, D., Betancur-R, R., Li, C., Becker, L., et al. (2018). Comprehensive phylogeny of ray-finned fishes (Actinopterygii) based on transcriptomic and genomic data 115, pp. 6249–6254. <https://doi.org/10.1073/pnas.1719358115>.
86. Close, R.A., Johanson, Z., Tyler, J.C., Harrington, R.C., and Friedman, M. (2016). Mosaicism in a new Eocene pufferfish highlights rapid morphological innovation near the origin of crown tetraodontiforms. *Palaeontology* 59, 499–514. <https://doi.org/10.1111/pala.12245>.
87. Paradis, E., Claude, J., and Strimmer, K. (2004). APE: Analyses of Phylogenetics and Evolution in R language. *Bioinformatics* 20, 289–290. <https://doi.org/10.1093/bioinformatics/btg412>.

## STAR★METHODS

### KEY RESOURCES TABLE

REAGENT or RESOURCE	SOURCE	IDENTIFIER
<b>Deposited data</b>		
Molecular Dataset (UCE sequence FASTAs and Chuanacid COI FASTA)	This study	Dryad Repository, GenBank
Fossil Calibrations	This study	Data S1 – Calibration List
Trait Data	This study	Dryad Repository
Molecular Reagents (>10)	Various	See “Method Details”
<b>Software and algorithms</b>		
BEAST2 Suite	Bouckaert et al. <sup>68</sup>	N/A
IQ-TREE	Nguyen et al. and Minh et al. <sup>19,20</sup>	N/A
Diversitree	Fitzjohn <sup>41</sup>	N/A
Phytools	Revell <sup>69</sup>	N/A
Tracer	Rambaut et al. <sup>70</sup>	N/A
ASTRAL	Zhang et al. <sup>23</sup>	N/A
Phyluce	Faircloth <sup>16</sup>	N/A
TOAST	Wcislo et al. <sup>21</sup>	N/A
CIAAlign	Tumescheit et al. <sup>18</sup>	N/A
ModelFinder	Kalyaanamoorthy et al. <sup>71</sup>	N/A

### RESOURCE AVAILABILITY

#### Lead contact

Requests for data should be made to [chase.brownstein@yale.edu](mailto:chase.brownstein@yale.edu).

#### Materials availability

All materials are available in the main text and the supplementary data on dryad. Newly sequenced UCE data is deposited on the NCBI Repository GenBank. Supplementary Figures displaying the ASTRAL III topology and additional summary statistics and plots are also available in the Dryad Digital Repository at: <https://doi.org/10.5061/dryad.9cnp5hqr>.

#### Data and code availability

All data and R code is deposited in the Dryad Digital Repository at: <https://doi.org/10.5061/dryad.9cnp5hqr>. We direct readers to the README file in the Dryad repository for more information.

### EXPERIMENTAL MODEL AND SUBJECT DETAILS

We created a new hypothesis of the phylogenetic relationships of anglerfishes and their timescale of diversification using maximum likelihood, multispecies coalescent, and Bayesian techniques on a dataset of 975 UCEs sequenced for 222 individuals.

### METHOD DETAILS

#### Taxon sampling and sequencing methods

In order to effectively sample lophioid diversity, we sequenced and aligned UCEs for 230 specimens of anglerfishes and 22 outgroups (2 individuals of *Antigonia capros* and 20 tetraodontoids representing all major clades)<sup>12,72</sup> from a bait set of 1,314 loci. *Lophichthys boschmai*, which traditionally comprises the monotypic *Lophichthyidae*, was not sampled. However, morphological analyses suggest that this species is nested within *Antennariidae*.<sup>73,74</sup> We follow the delimitation of families as presented in a phylogenetic-based and rank-free taxonomy of ray-finned fishes.<sup>75</sup> As such, our sampling comprises 100% of lophioid families, 66% of genera, and 25% of the species diversity in the clade. UCE data for 157 specimens come from previous studies.<sup>10,12</sup> New sequence data was generated largely following protocols outlined in previous phylogenomic analyses of acanthomorph teleosts.<sup>12,76</sup> We isolated DNA from muscle and fin tissue using Qiagen DNeasy Blood and Tissue kits, quantified 1 μL for each extraction using a Qubit fluorometer



(Life Technologies), confirmed successful isolation of high molecular weight DNA using gel electrophoresis, and sheared ~500 ng of DNA for each sample using a QSonix Q800R3 sonicator to produce sequence fragments ranging in length between 300 and 600 bp. Using Kapa HyperPrep kits (Kapa Biosystems) and Illumina TruSeq iTru5 and iTru7 adapters<sup>77</sup> and following the Kapa protocol for library preparation. We then sequenced the libraries using 150 bp paired-end sequencing on Illumina NovaSeq platforms after creating an equimolar pool of enriched libraries. We follow recent calls to italicize all formal taxonomic group names regardless of rank in Linnean-based classifications.<sup>75,78</sup>

### UCE sequence alignment, sanitation, and preprocessing

We used the phyluce 1.7.1 pipeline<sup>16</sup> to process raw reads, assemble sequences *de novo*, and construct UCE sequence alignments. We first used the phyluce pipeline to check for and remove potential paralogs. This produced 975 UCE alignments. All UCEs have been deposited on the NCBI repository GenBank under BioProject PRJNA1099172. Next, we conducted several additional analyses to identify and filter paralogous and chimeric sequences from our dataset. First, we used ClAlign<sup>18</sup> to flag and visualize chimeric or incorrectly included UCE sequences produced by phyluce. Next, we used custom scripts in the R package TOAST<sup>21</sup> to conduct a secondary screen for hidden paralogous genes and anomalously divergent sequences by checking for reciprocal monophyly of *Lophioidei* and the two outgroup clades (*Tetraodontoidae* and *Antigonia capros*). Finally, we tested for violations of common sequence substitution model assumptions, including stationarity, homogeneity, and reversibility, using scripts<sup>22</sup> implemented in IQ-TREE 2.2.03.<sup>19,20</sup> The final set of UCEs comprised 608 aligned loci for 222 individual specimens that comprise 124 species.

### Maximum likelihood phylogenetic analyses

All maximum likelihood phylogenetic analyses were conducted on the Yale High-Performance Computing McCleary and Farnam Clusters using IQ-TREE v. 2.2.0.<sup>19</sup> We conducted three separate maximum likelihood phylogenetic analyses that constructed final species trees using different methodologies. First, we inferred gene trees for individual UCE sequences using 1000 ultrafast bootstrap supports,<sup>79</sup> 1000 replicates of the Shimodaira-Hasegawa approximate likelihood ratio (SH-r) test, and models of nucleotide evolution for individual UCEs found using ModelFinder Plus.<sup>71</sup> These were summarized into a species tree using ASTRAL III v. 5.7.8.<sup>23</sup> Next, we divided the UCE alignments into 41 partitions using PartitionFinder2<sup>80</sup> and inferred a maximum likelihood topology with 1000 ultrafast bootstrap replicates. Finally, we inferred a maximum likelihood tree for the where the alignments were concatenated and treated as a single partition using 1000 ultrafast bootstraps and a model of nucleotide evolution inferred using ModelFinder Plus.<sup>71</sup>

### Concordance factors and anomaly zone detection

We measured the magnitude of gene tree-species tree discordance and site-species tree discordance by calculating gene (gCF) and site (sCF) concordance factors using IQ-TREE 2.<sup>19</sup> Values of gCFs measure the percentages of decisive gene trees consistent with particular branches in the partitioned tree topology, and sCFs measure the percentages of decisive alignment sites supporting branches in an input reference tree. We calculated sCFs using 100 subsampled quartets from our alignment and plotted gCF, sCF, bootstrap, and branch length values against each other to test for associations using R base code and tidyverse scripts ([http://www.robertlanfear.com/blog/files/concordance\\_factors.html](http://www.robertlanfear.com/blog/files/concordance_factors.html)). Examination of these plots revealed two regions of phylogenetic instability, one corresponding to most of the backbone divergences in Ceratioidea and another corresponding to genus-level divergences in Antennariidae. To further interrogate our data and locate discordant regions of our generated phylogeny, we used custom scripts on the ASTRAL-III species tree to test for the presence of anomaly zones at particular regions of the tree. Anomaly zones (AZs) can be detected by checking whether branch lengths scaled to coalescent units fall within theoretical boundaries for AZs<sup>17,31,32</sup>; we transformed branch lengths to coalescent units using quartet CFs before testing whether these branches were AZs using custom python code.<sup>31,32</sup>

### Divergence time estimation

We used a node-dating approach implemented in BEAST 2.6.6<sup>33,68</sup> to time-calibrate the phylogeny of lophioids using input xml files of the 15 longest partitions of UCE loci that we delimited using IQ-TREE 2. Input files were constructed using BEAUTi.<sup>33,68</sup> We used the general time reversible (GTR) model with gamma distributed among site rate variation (+G) model of nucleotide substitution, a relaxed log-normal molecular clock model, and the fossilized birth-death (FBD) model of divergence time estimation as implemented in BEAST 2.<sup>81</sup> For the FBD model, we specified rho as 0.25, which is the sampling fraction of all 408 recognized species of *Lophioidei* (following Eschmeyer's Catalogue of Fishes: <https://www.calacademy.org/scientists/projects/eschmeyers-catalog-of-fishes>) included in our dataset. We set the origin to 83.6 Ma as a uniform prior, which is the age of the oldest occurrences of fossils from the major crown percomorph clades (e.g., †*Gasterorhamphus zuppichinii*,<sup>12,72,82</sup> †*Nardoichthys francisci*<sup>83</sup>), with bounds of 145.0 Ma (Jurassic-Cretaceous boundary, marking the start of the fossil record and estimated ancestry of crown Acanthomorpha<sup>12,15,26,72,84,85</sup>) and 56.0 Ma (the oldest crown tetraodontoid fossils, marking the minimum age of the tetraodontoid-lophiod split).<sup>14,38,86</sup> The diversification rate parameter was set to 1.47, which is the number of lophiod species included in our dataset divided by the median age of the root origin prior, with bounds of 0 and 100.0. We used eleven fossil calibrations to node-date the tree, each of which are discussed in the Fossil Calibration Justifications section of the Supplementary Text. Each fossil calibration was placed using a lognormal MRCA prior such that 97.5% of the prior distribution fell before the fossil age. We fixed the tree topology to the maximum likelihood phylogeny from the partitioned IQTREE analysis of 608 UCE loci. For each partition, we ran

BEAST2 analyses for 200 million generations with a 10 million generation pre-burnin. Convergence of the posteriors was assessed using Tracer v. 1.7.1<sup>70</sup> and runs of the 11 partitions that converged were combined using LogCombiner 2.6.4 (subsampling every million generations)<sup>68</sup> and annotated to the target IQTREE topology using TreeAnnotator 2.6.6<sup>68</sup> using median node heights.

### Ancestral state reconstructions

We implemented two methods of discrete trait analysis to reconstruct the ancestral states in the evolutionary history of locomotory and reproductive modes in anglerfishes using the R packages ape<sup>87</sup> and phytools.<sup>69</sup> Reproductive modes were classified as temporary attachment, facultative parasitism (both temporary attachment and permanent fusion), obligate parasitism (permanent fusion only), or no reproductive parasitism. Data on locomotory and reproductive modes were taken from four primary studies.<sup>5–7,51</sup> We note that at least one study has argued that all ceratioids might be parasitic<sup>51</sup> and that temporary attachers are facultative species for which parasitism has not yet been observed. However, the genomic evidence and our ancestral state reconstructions of gene presence (Figure 3) suggests that at the very least, if this is true, the majority of anglerfishes would be facultatively parasitic without a degenerated genetic basis of major features of adaptive immunity. As such, we keep the standard classification of anglerfishes as either temporary, obligate, or facultative parasites. For data on sexual dimorphism, we assembled information on size differences in females and males from the literature<sup>5–7,40,50,51,74</sup> and categorized dimorphism as a binary character (significantly smaller males than females present/absent) and as a three-state character (no clear dimorphism, males smaller than females, males extremely small such that they are less than 33% the size of the females) and ran ancestral state reconstructions using both categorizations. In each case, we first used the fastAnc function in phytools to produce a rapid maximum likelihood estimate of ancestral states at nodes in the time-calibrated phylogeny. The make.simmap function in phytools was used to fit a continuous-time reversible Markov model on the evolution of reproductive mode and simulate stochastic character evolutionary histories over 1000 simulations using the Markov model and our inputted species trait data. The results were summarized on a single tree.

### Chaunacid mitochondrial gene tree and genetic distances

For most of the major lineages of anglerfishes, we are confident that our species sampling captures the node representing their most recent common ancestors. This is not true for Chaunacidae (sea toads). Although the UCE phylogeny includes one of the two valid chaunacid genera and 10 of 25 recognized species of *Chaunax*, we cannot be certain that our sampling has fully captured crown *Chaunacidae*. The time-calibrated UCE phylogeny indicates that crown *Chaunax* diversified recently relative to all other lophioid genera, so we suspected this genus is taxonomically over-split. These observations posed challenges to the use of a speciation-based branching model clade sampling fractions into relaxed clock and diversification analyses. We investigated the delimitation of sampled species of *Chaunax* by sampling sequences of the mtDNA gene COI for 11 of the 25 recognized species of *Chaunax* and one of four species of *Chaunacops* based on data available on GenBank. The COI DNA sequence alignment was analyzed using IQ-TREE with ultrafast bootstrap supports generated over 1000 replicates, 1000 replicates for the SH-r test, and model specification in ModelFinder Plus. The resulting phylogeny was rooted on *Chaunacops coloratus*. Finally, we imported the COI DNA sequence alignment into R and calculated pairwise genetic distances among species of *Chaunacidae* using the R package ape.

### Trait-based species richness and diversification rates

We conducted several tests for associations between species richness and reproductive and locomotor traits in lophioids. First, we used chi-square tests implemented in R to investigate associations between species richness, reproductive mode, locomotory mode, and habitat in anglerfishes. Species diversity reflected the number of recognized species reported in Eschmeyer's Catalogue of Fishes and categorized for each trait state by reviewing the literature.<sup>11,13,24,51</sup> From these data, we constructed a four-by-three table listing the number of species displaying each of four reproductive modes: no sexually parasitic reproductive mode (1), sexually parasitic reproductive mode (2), and temporary attachment (3); and three different habitat modes based on data from FishBase.se: (1) shallow water benthic (<200 m), (2) deep water benthic (>200 m), and (3) bathypelagic (open water of the deep ocean, approximately 1 to 4 km below surface). We used the Rstats function chisq.test to run  $\chi^2$  and examined expected, observed, and residual values. Next, we conducted trait-dependent diversification rate analyses using the R package diversitree<sup>41</sup> using MuSSE (multistate dependent diversification rate analysis) models for the reproductive and locomotory mode character sets. We tested for differences in diversification rates associated with locomotory modes by running a BiSSE (binary state dependent diversification rate analysis) on locomotory mode characterized as either demersal or open-water-swimming. For the MuSSE analyses of the whole sample, reproductive mode was categorized as either (1) no sexual parasitism, (2) true sexual parasitism, or (3) temporary attachment; for MuSSE analyses on reproductive mode among ceratioids and locomotory mode, trait categories were the same as those in the  $\chi^2$  tests. In each SSE analysis, sampling fractions for each trait were set based on the number of species represented in the phylogeny relative to the clade species diversity reported in Eschmeyer's Catalogue of Fishes. In BiSSE, we tested likelihood models where speciation rates were the same or allowed to differ. In MuSSE, we compared the fits of six different likelihood models variously constraining trait transition rates, speciation rates, and extinction rates to our three-state trait sets using AIC scores. For the best-fit model in each case (the model with the lowest score), we ran an MCMC chain for 10,000 generations with sampling every 100 generations, discarded the first 1000 samples as burn-in, checked for convergence by examining caterpillar plots of log likelihood scores per generation, and plotted net diversification rate distributions and transition rates among states.

### Evolutionary history of anglerfish immunogenetics

Some genetically nonidentical male and female anglerfishes have the ability to fuse because they have degenerated genetic bases for vertebrate adaptive immunity.<sup>11</sup> To reconstruct the variance in anglerfish immunogenetics and investigate the evolutionary history of these genomic losses, we compiled data on the immunogenetics of key clades *Lophioidei* from recent studies.<sup>46,48</sup> Genes were chosen due to their well-known functionality in vertebrates including fishes and their central role in mediating or enabling the adaptive immune response. This approach allowed us to fill in a table of anglerfish immune gene losses, pseudogenizations, and other modifications. Using these data, we inferred the presence of key features of the adaptive immune system in a subset of anglerfishes and conducted ancestral state reconstructions in the R packages ape<sup>87</sup> and phytools<sup>89</sup> for the following: cytotoxic T-cells, helper T-cells, B-cell antibodies, and B-cell affinity maturation. We coded three states for each: present, absent, and present but pathway degraded/receptors missing as in a previous study.<sup>11</sup> We used fastAnc as a first-pass reconstruction followed by make.simmap to fit continuous-time reversible Markov models and simulate stochastic character evolutionary histories over 1000 simulations.

### QUANTIFICATION AND STATISTICAL ANALYSIS

See ‘Method Details’ for specific information and the [Key Resources Table](#) for software used.  $N = 230$  anglerfish individuals and  $N = 22$  outgroups were sequenced for UCEs.